Defects in *a*-Si and *a*-Si:H: A numerical study

Simone Knief and Wolfgang von Niessen
Institut für Physikalische und Theoretische Chemie, Technische Universität Braunschweig, Hans-Sommer-Straße 10, D-38106 Braunschweig, Germany

Thorsten Koslowski
Institut für Physikalische Chemie und Elektrochemie I, Universität Karlsruhe, Kaiserstraße 12, D-76128 Karlsruhe, Germany
(Received 30 September 1997; revised manuscript received 12 May 1998)

We present a numerical study of the electronic properties of various structural models of amorphous silicon and hydrogenated amorphous silicon. Starting from an ideal random network, dangling bonds, floating bonds, double bonds, microvoids, hydrogenated dangling bonds, and hydrogenated floating bonds are introduced. The concentrations of these defects can be varied independently, the amount of disorder introduced to the system is therefore strictly controllable. Two continuous random networks, the vacancy model of Duffy, Boudreaux, and Polk and the bond switching model of Wooten, Winer, and Weaire (WWW model) are investigated. For the relaxation of the structures the potentials of Keating and of Stillinger and Weber are employed. The electronic structure is described by a tight-binding Hamiltonian; the localized or extended character of the eigenstates is investigated via a scaling approach. The vacancy model shows a band gap for small defect concentrations but this fills up with increasing disorder. Similar behavior is found for the case of the other models. In general defects introduce states into the gap region of *a*-Si, where the dangling bonds lead to the largest density of states in the gap region for a given defect concentration. This model turns out to be unique. For small system sizes an impurity band results that dramatically changes its character for large systems above 4000 atoms to a nearly uniform density of states as observed experimentally. In *a*-Si:H the dangling and floating bonds are removed and a mobility gap results with a width in good agreement with experiment. The experimentally observed tailing of the band into the gap region (first linear, then exponential) is well described only for the *a*-Si:H model derived from the vacancy model and for very large system sizes above 4000 atoms. The WWW model does not lead to this tail behavior. Localized states are found at all band edges but states at the bottom of the conduction band are more strongly localized than those at the top of the valence band.
[S0163-1829(98)00532-3]

I. INTRODUCTION

Over the past twenty years, considerable effort has been devoted to the understanding of the properties of amorphous silicon (*a*-Si) and hydrogenated amorphous silicon (*a*-Si:H). These systems are particularly interesting due to potential technical applications. Modeling the microscopic and the electronic structure of *a*-Si and *a*-Si:H has, however, remained a considerable challenge in the field of computational solid-state physics. A variety of models have been introduced to describe the microscopic geometry of these systems. These are either based upon continuous random networks [1–5] (CRN's) or molecular-dynamics (MD) simulations.[6–13] The latter utilize empirical potentials[6–11] or apply *ab initio* simulation techniques.[12,13] Recently, structural models based upon quasicrystals have been introduced.[14,15]

In an ideal CRN, all atoms retain their normal coordination number $Z=4$, and deviations from crystalline bond lengths and bond angles are small. For *a*-Si, however, ESR experiments have demonstrated that 1–2 % of all atoms have to be characterized by a coordination number different from four. Although models based upon CRN's do not take these results into account, this type of structural model is able to reproduce some of the essential features of the electronic structure, namely, the width of the valence band and the principal structure of the density of states (DOS).[16,17]

For *a*-Si the valence-band (VB) density of states consists of two peaks and the conduction band (CB) is nearly featureless. Calculations of the electronic properties of *a*-Si based on a CRN have been performed by several authors.[18–21] This type of structural model is not able to reproduce the DOS in the vicinity of the Fermi level because it leads to a true gap between the two energy bands and this is not consistent with experimental results. Nevertheless a CRN is a simple model to study the influence of topological disorder—i.e., the presence of five- and seven-membered rings in addition to six-membered rings characterizing the crystalline state — on the electronic properties of covalently bonded amorphous systems. In this paper we study the influence of different degrees of topological disorder on the electronic structure and the localization behavior of electronic eigenstates for two different CRN's [the vacancy model of Duffy, Boudreaux, and Polk[4] and the bond switching model of Wooten, Winer, and Weaire[1] (WWW)].

In contrast to CRN's, structures that are generated by MD simulations of rapid quenching contain dangling and floating bonds. Their exact concentration is difficult to control, and the number of different types of defects can not be varied independently. Most of the structures presented in the literature contain a larger number of floating than dangling bonds, with the exception of the model developed by Biswas, Grest, and Soukoulis.[6] In general, the concentration of undercoor-

dinated and overcoordinated atoms in models generated by MD simulations lies above the experimental one. System sizes are usually limited to only a few hundred atoms; *ab initio* simulations are limited to even smaller system sizes and to a small number of realizations. Holender and Morgan have constructed large systems (up to 13 824 atoms) by assembling small simulation cells, followed by a relaxation procedure using a classical interaction potential. Schmitz, Peters, and Trebin[14] have investigated the suitability of a tetrahedral quasicrystal to describe both the structural and the electronic properties of amorphous silicon. Their models contain up to 20.000 atoms and a fraction of 0.0156 atoms with $Z=3$, which is close to the experimental value.

Whereas the electronic structure of a CRN shows a clear gap between the two energy bands for small degrees of topological disorder, the presence of dangling and floating bonds leads to the shift of eigenstates into the vicinity of the Fermi level.[19,21] States around the Fermi level are usually believed to be localized. This disorder-induced Anderson localization leads to the formation of a mobility gap containing eigenstates not participating in electronic transport at zero Kelvin. Mobility edges E_C and E_V separate localized from extended states. The DOS outside the gap region is similar for a CRN and a defect structure. The introduction of hydrogen — leading to the formation of *a*-Si:H — has a strong effect on the electronic structure. The books of Joannopoulus and Lucovsky[16,17] and Street[22] present a good overview of the theoretical and experimental properties of *a*-Si:H. On account of the technical importance of *a*-Si:H numerous theoretical investigations have been performed to understand the role of hydrogen in the amorphous state.[23–33] Compared to *a*-Si the defect concentration in *a*-Si:H is drastically reduced. It has been observed experimentally that only one out of 10^7 atoms shows a coordination number different from four for a concentration of 20 at. % hydrogen. (Amorphous silicon prepared by various methods can obtain up to 40 atomic percent hydrogen, but for photovoltaic devices the content of hydrogen is in the range of 10–20 %.) The introduction of hydrogen removes most of the states from the gap region[23] and induces the widening of the mobility gap from 1.5 eV in *a*-Si to 1.8 eV in *a*-Si:H as found experimentally.[34] In addition, *a*-Si and *a*-Si:H differ in the positions of the band edges and the structure of the upper region of the VB. For the hydrogenated form the maximum of the VB lies at lower energies compared to *a*-Si and c-Si. The band edges in the gap region recede with increasing hydrogen concentration. This effect is stronger at the top of the VB than at the bottom of the CB. As in the case of *a*-Si most of the structural models for *a*-Si:H presented in the literature contain only a few hundred atoms with the exception of the model developed by Holender, Morgan, and Jones.[23] It contains 1545 silicon atoms and 450 hydrogen atoms, i.e., the hydrogen content is about 22%.

Although the properties of amorphous silicon have been studied intensively over the last 20 years, some important aspects are not yet clarified. One is the question of which type of defect is dominant in *a*-Si. It is generally proposed that dangling bonds represent the major type of defect.[35–38] Pantelides[39,40] on the other side has suggested that floating bonds form the dominant type of defect. Mercer and Chou[41] as well as Biswas *et al.*[19] have tried to clarify this aspect by the calculation of the local density of states (LDOS) for atoms with different coordination numbers for model systems that contain both types of defects. They both find, that the presence of threefold-coordinated atoms create more states in the vicinity of the Fermi level than the presence of floating bonds does. To address this question we have developed structural models that contain only one type of defect (either dangling bonds, floating bonds, double bonds, or microvoids) and have calculated both the density of states and the LDOS for these structures. In addition, we have studied the interdependence of different types of defects existing in the same structural model.

For a better understanding of the amorphous state it is essential to compute the localized or extended character of eigenstates besides the DOS. The localization character is required to determine the value of the mobility gap as compared to the band gap. It is well accepted that localization is only present at the band edges and is stronger in the conduction band than in the valence band. The numerical value of the mobility gap has been computed by Holender and Morgan[42] and Schmitz and co-workers.[14] Holender and Morgan have studied the localization behavior of the electronic states for *a*-Si and *a*-Si:H using the inverse participation ratio (IPR) and find a mobility gap of 1.2 eV for *a*-Si and 1.8 eV for *a*-Si:H. Schmitz and co-workers have calculated the localization behavior of different structural models containing only silicon atoms utilizing two different criteria (the participation ratio and the localization length). They find mobility gaps that lie between 1.33 and 2.0 eV. An additional aspect that has not been discussed in detail up to now is the structure of the band tails. Total yield photoelectron spectroscopy shows that in *a*-Si:H the band edge of the VB consists of two parts[43]: first it falls off linearly and than tails exponentially into the gap region. The valence-band tail is wider than the tail of the conduction band.[44,45] Most of the structural models presented in the literature are not able to reproduce this experimental observation for the simple reason that they only contain a few hundred atoms. Whereas Holender and Morgan make no prediction about the detailed structure of the band edges in their structural model, Schmitz and co-workers have observed the presence of the exponential decrease of the band edges.

In the present paper we discuss the DOS and the localization character of states for different structural models for *a*-Si and *a*-Si:H. As will be demonstrated below, to arrive at a reliable statement about the location of the mobility edges E_V in the VB and E_C in the CB and to reproduce the behavior of the band tails a scaling analysis including system sizes up to 10 000 atoms turns out to be essential.

For technical application of amorphous semiconductors the knowledge of the electronic properties is imperative. On the other hand, for a detailed understanding of the amorphous state the computation of both the electronic and the vibrational properties is required. The investigation of the vibrational density of states and the localization behavior of these states for several structural models studied in this paper has been performed by Finkemeier and von Niessen and is presented in an accompanying paper.[46] The comparison of the results of the electronic and the vibrational properties leads to the conclusion that some structural models are more suitable to describe the electronic properties, whereas other

models are able to reproduce the vibrational properties in a better way. The influence of topological disorder and of the different types of defects on the DOS and the localization character of the states is stronger for the electronic than for the vibrational properties. The next two sections contain a detailed description of the different structural models and the methods that are used to calculate the electronic DOS and the localization character of the states. Results are presented and discussed in Sec. IV. Conclusions are derived in the last section.

II. MODEL CONSTRUCTION

In this paper two different CRN's are used to describe the structure of amorphous silicon: the vacancy model of Duffy, Boudreaux, and Polk[4] and the bond switching model of Wooten, Winer, and Weaire.[1] These models have been applied previously to the calculation of the electronic properties of a-Si.[18–20] These, as all other models that are described in this paper, contain periodic boundary conditions to avoid surface effects.

In the vacancy model topological disorder is introduced by removing a certain number of atoms randomly from the diamond structure. After each elimination the four unsaturated atoms have to be reconnected by new bonds. Detailed information about the construction of this type of CRN is given by Duffy, Boudreaux, and Polk[4] and Koslowski and von Niessen.[20] The degree of disorder in this structural model can be measured by the vacancy concentration, c_f. This is the fraction of atoms that is removed from the regular diamond lattice. Afterwards the lattice is relaxed using a Monte Carlo (MC) procedure[20] with the Keating potential.[47] During the relaxation process the energy of the network is minimized subject to the condition that the average bond length is the same as the crystalline one. The resulting CRN structure that best describes the experiment shows a density that is about 8% higher than the density of c-Si. In general the calculations are performed for this density, no strong dependence of the electronic properties on the density has been detected in the range of $0.9\rho(c\text{-Si}) \leqslant \rho \leqslant 1.10\rho(c\text{-Si})$.

In contrast to the vacancy model the CRN that is based on the bond switching model contains the same number of atoms as the original diamond lattice. The topological disorder is introduced by switching a given number of existing bonds. A detailed description is given by Wooten, Winer, and Weaire.[1] To keep deviations from the crystalline bond angle small some rules for the exchange of bonds are introduced. Only bonds that show the same length as in the crystal can be switched and the resulting structure is not allowed to contain four-membered rings. The CRN that is realized via this procedure has the same density as the original diamond lattice. We have found no significant dependence of the electronic properties on the density within physically reasonable variations of ρ. The degree of disorder can be varied by the number of bonds that are switched. To compare the results of different system sizes we have introduced a dimensionless factor c_n, defined as the percentage switched bonds with reference to the number of atoms in the lattice. In addition to the six-membered rings that are present in the diamond lattice five- and seven-membered rings are created in the disordered structure, a feature similar to the vacancy model.

The vacancy model of Duffy, Boudreaux, and Polk[4] is the starting point for the development of structural models which contain only one type of defect with a given concentration. To introduce dangling bonds the longest bonds are cut. The resulting structure is relaxed using the MC method mentioned above with an updated connectivity list. In this way we are able to realize dangling bond concentrations up to 20%. It is assumed that the Keating potential that has been developed for tetrahedral systems is appropriate for this and subsequent structural models.

To introduce fivefold and sixfold coordinated atoms we start from the diamond lattice instead of a CRN. A large local vacancy concentration has been found to give rise to floating bonds. We thus remove four instead of only one atom from the regular lattice for each elimination step. These four atoms are a randomly chosen particle and three of its twelve second-nearest neighbors, which are also chosen at random. The formation of the new bonds and the relaxation process are performed using the procedure above. To generate a neighborhood list it is necessary to define a cutoff radius for the nearest-neighbor shell. We use a cutoff of 3.1 Å.

Most structural models introduced in the literature are generated via molecular-dynamics simulations using the Stillinger-Weber potential.[48] All of these structures contain both dangling and floating bonds, but the concentration of these cannot be controlled. To study the influence of different types of defects in the same structure we have developed a model that contains dangling and floating bonds in arbitrary relations. We start from the dangling bond model and introduce the floating bonds via the procedure mentioned above.

In contrast to a-C double bonds play a negligible role in the amorphous state of silicon. Nevertheless this type of defect might lead to typical changes in the electronic properties. To develop a structural model that contains this type of defect in variable concentrations, we start from the diamond lattice. To generate a double bond between two neighboring atoms A and B, one neighbor of A and one of B, chosen randomly, are removed from the regular lattice in each elimination step. After this step the unsaturated atoms are connected with each other. In this way the atoms A and B will be connected by a single σ and a π bond. Subsequent to this procedure the length of the double bonds is reduced to 2.15 Å. This is close to the value that a silicon double bond shows in most inorganic materials. This value of the bond length as an average value has to be taken into account in the subsequent relaxation process as a constraint.

All structural models described so far are relaxed with the Keating potential. In addition, we have generated structures for the vacancy model and for the bond switching model where the relaxation has been performed using the Stillinger-Weber or the Tersoff potential.[49] A detailed description of the relaxation method together with the Stillinger-Weber potential is given in the accompanying paper by Finkemeier and von Niessen.[46] To calculate the electronic properties we use in most cases a cutoff for the nearest-neighbor shell of 2.8 Å. Atoms beyond this distance are considered not to be bonded in the tight-binding Hamiltonian.

A further aspect of our work is the examination of the changes in the electronic properties when the different types of defects are partially or completely removed by hydrogen.

To achieve this we have developed two different models for *a*-Si:H. They are based on the dangling bond model or on the floating bond model. To introduce hydrogen to a defect structure we use the method suggested by Holender and Morgan.[23] In this procedure all atoms that display a coordination number different from 4 are removed from the lattice. The resulting free bonds can partially or completely be saturated with hydrogen atoms. The Si-H distances are assumed to be the same as in SiH_4, i.e., 1.48 Å. Following Guttman[25] we use the Keating potential to relax the *a*-Si:H structure. The relationship between the two Keating parameters, α and β is as follows: $\beta = 0.30\alpha$, but $\alpha(H) = 2\alpha(\mathrm{Si})$ as suggested by Guttman.[25] In this structural model most of the hydrogen atoms are bonded within SiH_1 groups. With increasing hydrogen concentration the amount of SiH_2 groups increases and only for the highest concentration of hydrogen a few SiH_3 groups exist. The present *a*-Si:H model disregards the formation of Si-H-Si bonds.

The *a*-Si:H structure is the starting point for the development of a model that contains microvoids of arbitary size and concentration. To create such a void all particles in the neighborhood of a randomly chosen atom are removed until the desired size of the microvoid is obtained. The resulting free bonds are now partially or completely saturated with hydrogen atoms.

III. NUMERICAL APPROACH

To calculate the electronic structure we use the tight-binding method. It is the only method that permits us to treat the required large system sizes of thousands of atoms. This technique requires only information about the short-range order. For the vacancy model we have investigated the suitability of four different tight-binding parametrizations that can be found in the literature. Two of them assume a basis of one *s* and three *p* orbitals. The basis is considered to be orthogonal on and among the atoms. They have been developed by Chadi and Cohen[50] and Harrison.[51] These two parameter sets include only interactions between nearest neighbors. The presence of different bond lengths is taken into account via the $1/r^2$ scaling as suggested by Harrison.[51] The deviations in the bond angles are treated in the formalism of Slater and Koster.[52]

The parameter set of Vogl, Hjalmarson, and Dow[53] includes an additional s^* orbital. In this parameter set only interactions between nearest neighbors are considered. The differences in the bond lengths are also taken into account.[54]

The parameters of Allen, Broughton, and McMahan[55] are an example for a nonorthogonal tight-binding set. An application of these parameters to the calculation of the DOS of *a*-Si is given in the work of Mercer and Chou.[41] In this tight-binding approach interactions up to the third-neighbor shell are included, provided the distances between two atoms are smaller than the cutoff of 4.7 Å.

For our structural model we have found, in a comparison with experiment, that the parameter set of Harrison is the most suitable one to describe the essential features of the electronic properties of *a*-Si. The results obtained with the parameters of Chadi and Cohen are very close to them. Therefore the calculations of the defect structures are performed with the tight-binding set of Harrison only.

The use of the parameter set of Vogl, Hjalmarson, and Dow leads to the following differences compared to experiment and the results with a minimal orthogonal tight-binding basis: (a) The VB is slightly too wide compared to experiment. (b) The two lower peaks of the VB tend to merge at the transition from the crystalline to the amorphous state, but for a realistic degree of topological disorder the two lower peaks are not completely washed out. (c) The width of the upper peak of the VB is in good agreement with experiment. (d) The CB is featureless only for system sizes exceeding 1500 atoms. (e) The energy gaps are smaller. (f) The mobility gap is too large.

We are only able to calculate the electronic structure using the tight-binding approach of Allen, Broughton, and McMahan[55] for structures with a vacancy concentration smaller than $c_f = 0.10$. For a higher degree of disorder negative eigenvalues of the overlap matrix are obtained. The reason for this behavior lies in the fact that the deviations from the mean value of the bond lengths are so large that not all of the first-, second-, and third-nearest neighbors fall into the fitting range of the polynomials from 2.3 Å to 4.7 Å. Thus this approach is not suitable for *a*-Si.

In the calculation of the electronic properties of the *a*-Si:H structures we have compared two different parameter sets. One of them has been developed by Allan and Mele[56] and the other one by Min *et al.*[31] We have found (compared with experiment) that the tight-binding approach of Allan and Mele appears to be more suitable to describe the properties of *a*-Si:H in our model. This parameter set was also used by Holender, Morgan, and Jones[23] in their calculations.

To study the localization behavior of the electronic states we apply three different criteria. These are the inverse participation ratio (IPR),[57] the correlation length[58,59] and a method which was developed by Thouless, Edwards, and Licciardello (TEL method).[60–62] The last criterion has the advantage that only the eigenvalues are required to predict the localization character. The correlation length and the TEL method are used as a scaling procedure, i.e., the electronic structure has to be calculated for different system sizes with the same degree of disorder.

The main disadvantage of the IPR is that it does not permit us to calculate the position of the mobility gap in a straightforward way. But this problem can be circumvented in a pragmatic way by taking recourse to the other approaches. As we found little differences between the results obtained by these approaches we present the TEL method in some more detail and give the results obtained in this way below. A more detailed discussion of the relevant approaches and results for the case of phonon localization is given in the companion paper.[46]

Thouless, Edwards, and Licciardello have pointed out that the energy of a localized state is nearly independent of the choice of the boundary conditions, whereas extended states are sensitive to the boundary conditions. To determine the localization character using the TEL method it is necessary to calculate the eigenvalue spectrum with two different types of boundary conditions. Whereas Thouless, Edwards, and Licciardello employed periodic and antiperiodic boundary conditions, we make use of periodic and weakly decoupled boundary conditions in one spatial direction. This idea is taken from the article of Koslowski and von Niessen.[20] For

the choice of the magnitude of the decoupling factor two conditions exist. First, the decoupling factor has to be sufficiently small to lead to a shift of the eigenvalues smaller than the average level spacing. Otherwise it would be difficult to map the two spectra for different boundary conditions. Second, the accuracy of the procedure that is used to calculate the eigenvalues presents a lower boundary of the decoupling factor. In our investigations we have found no changes in the localization behavior of the electronic states if the value of the decoupling factor lies between 10^{-2} and 10^{-4}. The results presented in this paper are computed using a decoupling factor of 10^{-3}. To deduce the localization character of the electronic states using the TEL method the so-called Thouless number $g(l)$ has to be calculated:

$$g(l)=\frac{\Delta E}{\partial E}. \tag{1}$$

In this equation l denotes the system size (linear dimension), ∂E is the average energy difference between two levels in a given energy bin, and ΔE is the average difference between the corresponding eigenvalues for the two sets of boundary conditions. The average is taken over small energy intervals and over different realizations. To compare the results for different system sizes, we calculate the negative natural logarithm of the Thouless number. For extended electronic states the value of $-\ln g$ decreases with increasing system size. An increasing value of $-\ln g$ with increasing system size indicates localized electronic states.

The calculation of the electronic structure with an orthogonal tight-binding approach leads to a large sparse matrix. To compute the eigenvalues and eigenvectors the Lanczos algorithm is used.[63–65] For system sizes smaller than $N=8$ (4096 atoms) the DOS is studied for the entire energy range. As the presence of localized states in the interior of the two energy bands has not been observed, the analysis of the localization character for the larger systems has been limited to the band edges around the Fermi level. For the various structural models the number of realizations lies between 100 ($N=3$, 216 atoms) and 3 ($N=12$, 13 824 atoms). Most of our calculations of the defect structures are performed with a vacancy concentration of $c_f=0.10$, because at this degree of disorder the radial distribution function (RDF) of the vacancy model shows the best agreement with the experimental one. Defect concentrations, c_d, of 1.11%, 2.22%, 11.11%, and 20% have been considered. If we remove all defects from the a-Si structure via hydrogenation the resulting a-Si:H structures contain 6.39, 12.24, 21.43, and 42.85 atomic percent hydrogen, respectively.

IV. RESULTS AND DISCUSSION

A. Structural aspects

The radial distribution functions (RDF's) and the distribution of bond lengths and bond angles are discussed in some detail in the second paper.[46] We thus omit a discussion here. It should be said that the best agreement of the RDF with experiment is obtained for a vacancy concentration of $c_f=0.10$ and a bond switching parameter of $c_n=0.15$ to 0.20. In case the Stillinger-Weber potential is used this parameter should be increased to $c_n=0.20$ to 0.25. The defects have the following effects on the RDF: the floating bonds cause nearly no change; the dangling bonds have a noticeable effect only for a defect concentration exceeding 11%, then a third maximum appears; the double bonds cause a shift of the minimum between the peaks to larger distances. The RDF's of a-Si:H show a reasonable agreement with the experimental curves[66] and with the results of other structural models.[29,30,23]

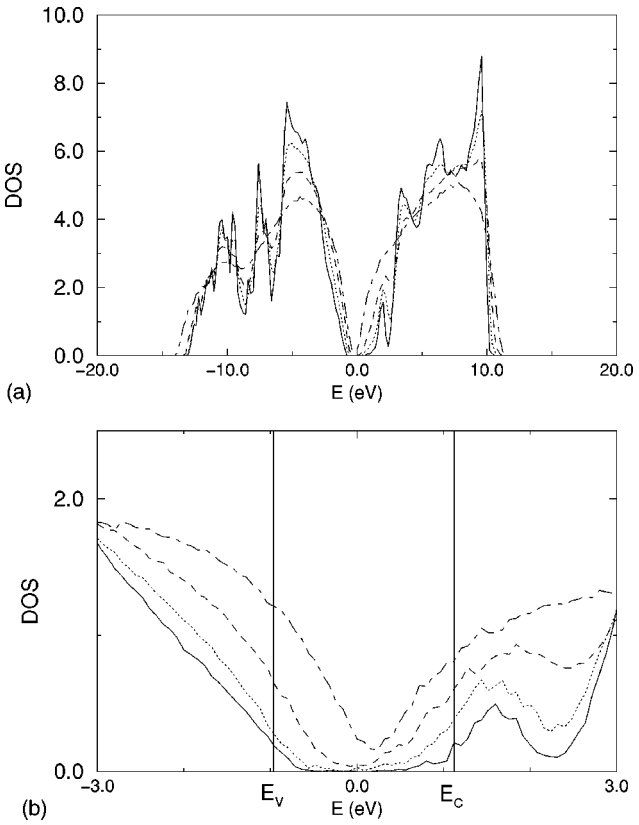

FIG. 1. Density of states for the vacancy model (solid line, $c_f=0.025$; dotted line, $c_f=0.05$; dashed line, $c_f=0.10$; dash-dotted line, $c_f=0.20$). (a) $N=6$ (1556 atoms), (b) $N=10$ (7200 atoms).

B. Vacancy CRN model

To study the influence of the structural disorder on the electronic properties we have used four different vacancy concentrations $c_f=0.025$, 0.05, 0.10, and 0.20. The resulting electronic densities of states are shown in Fig. 1. The energy resolution has been chosen as 0.2 eV per energy interval in view of the great width of the VB and the CB. The figures that show the DOS in the vicinity of the Fermi level have a resolution of 0.1 eV. In the calculation of the localization character we have used a resolution of 0.1 eV. The figures display the computed mobility edges E_V and E_C for a degree of disorder of $c_f=0.10$ and a defect concentration of dangling bonds, floating bonds, or double bonds of $c_d=2.22\%$. The mobility edges are certainly shifted by varying the degree of disorder but this effect is in general too small to be visualized. This is why the information is only given for the most relevant defect concentration.

Whereas for the smallest vacancy concentration the VB consists of three peaks, the two upper peaks merge with increasing disorder. For the most relevant vacancy concentra-

TABLE I. Mobility gaps in eV for the two CRN's with different degrees of disorder.

Vacancy model	$c_f=0.025$	$c_f=0.05$	$c_f=0.10$	$c_f=0.20$
Mobility gap	2.8	2.5	2.0	0.8
WWW model	$c_n=0.10$	$c_n=0.15$	$c_n=0.20$	$c_n=0.25$
Mobility gap	2.5	1.7	0.9	0.8

tions the CB is featureless. With increasing topological disorder the energy gap between the VB and the CB decreases. For a vacancy concentration of $c_f=0.20$ this gap disappears and the gap slowly fills up, but the DOS in this region remains small. We find that the width of the energy gap decreases with increasing system size at a constant degree of disorder. The structure of the interior of the two energy bands shows, on the other hand, no dependence on the system size. To describe the band tails properly it is necessary to calculate systems that contain more than 4000 atoms. Figure 1(b) shows the DOS around the Fermi level for a system with $N=10$ (8000 atoms) for various vacancy concentrations. If the degree of disorder is smaller than or equal to $c_f=0.10$ one obtains a linear behavior of the band tails. The exponential tail is only clearly apparent for the smallest vacancy concentration. There is still a lot of noise superimposed on this part of the tail behavior that is, however, definitely different from the linear region. Much larger system sizes would have to be studied to find the tailing behavior in this region of very low DOS.

For all structural models that are discussed in this paper we find localized states only at the band edges. For a vacancy concentration of $c_f=0.025$ no localized states exist at the bottom of the VB, but the number of localized states increases in this region with increasing disorder. Localization at the top of the CB occurs for all degrees of disorder and its amount increases with increasing vacancy concentration. At the bottom of the conduction band we find localized states for all degrees of disorder, but their total number decreases with increasing disorder. At the top of the VB localized states are observed only if the vacancy concentration is smaller than $c_f=0.20$. Stronger localization at the CB edges than at the VB edges is found for all degrees of disorder. This result agrees with the investigations of other authors.[18,20,42,14] It also agrees with other experimental investigations.[67] The DOS shows an asymmetry in the band edges in the gap region, i.e., for a given energy above and below the Fermi level the DOS is higher in the VB than in the CB. This feature was also observed by Nichols and Winer and can explain the stronger localization in the CB than in the VB. The width of the mobility gap is an important feature for a comparison with experiment. For the vacancy model the values of the mobility gaps are listed in Table I. With increasing structural disorder the width of the mobility gap decreases, but for realistic vacancy concentrations the value is larger than the experimental one of 1.5 eV. To conclude, the DOS calculated for a vacancy concentration of $c_f=0.10$ agrees best with experimental results. This holds also for the phonon density of states.[46]

C. Bond switching CRN model

The results for the bond switching model (WWW model) agree in many respects with those of the vacancy model (see Fig. 2). For this model the two energy bands lose their structure with increasing disorder and the number of states around the Fermi level increases. In contrast to the vacancy model the energy gap disappears already for a small degree of disorder (results not presented here), but the number of states around the former gap remains small in comparison to the interior of the two bands. This structural model leads to a stronger localization at the two edges of the CB than of the VB and the number of localized states increases with disorder. If the degree of disorder is larger than $c_n=0.15$, localization at the top of the VB is completely suppressed. The values for the mobility gaps are listed in Table I. The bond switching model is not able to describe the partition of the band tails into a linear and an exponential part for any system size. In particular, the linear part is found for no degree of disorder, whereas it is clearly apparent for a wide range of the disorder parameter in the case of the vacancy model.

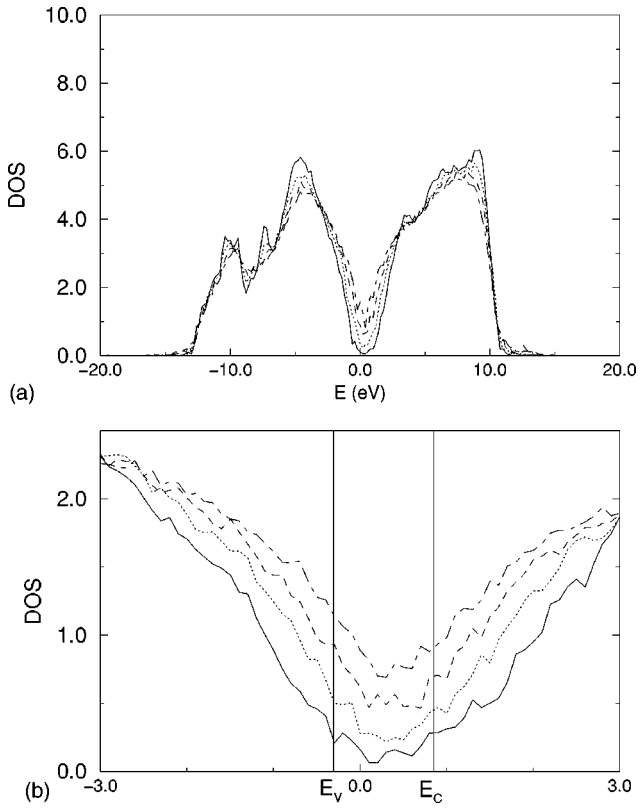

FIG. 2. Density of states for the WWW model in the case of relaxation with the Keating potential (solid line, $c_n=0.10$; dotted line, $c_n=0.15$; dashed line, $c_n=0.20$; dash-dotted line, $c_n=0.25$). (a) $N=6$ (1728 atoms), (b) $N=8$ (4096 atoms).

D. Dangling bond model

The introduction of dangling bonds into the CRN causes strong changes in the DOS only in the vicinity of the Fermi level. In the other energy regions we have found no significant differences compared to the vacancy CRN model. Figure 3 shows the DOS for this structural model in the region of the Fermi level. Due to the presence of threefold-coordinated silicon atoms the energy gap between the VB and the CB disappears and the number of states in this region increases with increasing defect concentration. Around the Fermi level the DOS shows features that vary dramatically

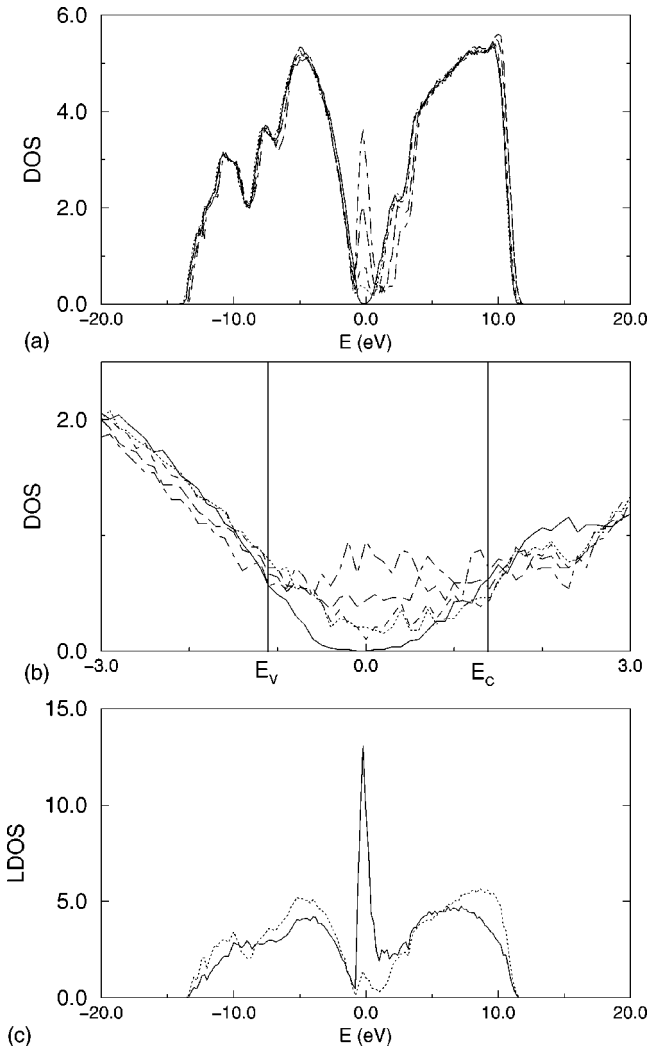

FIG. 3. Density of states (DOS) and local density of states (LDOS) for the dangling bond model. (a) DOS, $N=6$ (1556 atoms) (solid line, $c_d=0\%$; dotted line, $c_d=1.11\%$; dashed line, $c_d=2.22\%$; long-dashed line, $c_d=11.11\%$; dash-dotted line, $c_d=20.0\%$). (b) DOS, $N=8$ (3688 atoms) (solid line, $c_d=0\%$; dotted line, $c_d=1.11\%$; dashed line, $c_d=2.22\%$; long-dashed line, $c_d=11.11\%$; dash-dotted line, $c_d=20.0\%$). (c) LDOS, $N=5$ (900 atoms), $c_d=11.11\%$ (solid line, threefold-coordinated atoms; dotted line, fourfold-coordinated atoms).

with system size. If the system contains less than 2000 atoms, the presence of dangling bonds gives rise to an additional peak whose intensity increases with increasing defect concentration. The maximum of this peak lies below the Fermi level and moves to lower energies with an increasing number of threefold-coordinated atoms. The explanation for this effect that the Fermi level does not coincide with the maximum of the impurity band is simply that we do not have a half-filled dangling bond impurity band. In all models the most general hybridization is permitted. For larger system sizes this peak disappears. Although the appearance of this beautiful impurity band may be pleasing, it is a finite-size effect persisting up to about 2000 atoms. For larger systems (above about 4000 atoms) the introduction of dangling bonds leads only to a featureless increase in the number of states between the two energy bands. This structure of the DOS is in better agreement with the experiment than the formation of the peak described above. With this and the other defect structural models we do not find the tailing behavior discussed above. This is apparently restricted to the vacancy CRN model.

Like our model the structural model developed by Schmitz[15] contains only fourfold- and threefold-coordinated atoms. In his model the formation of dangling bonds lead to states in the vicinity of the Fermi level but these states are more or less isolated from the bulk of the states in the two energy bands. He finds no states between the top of the VB and the impurity band and only a small number of states between the gap states and the CB. The impurity band is split. Schmitz suggested that this partition is caused by the formation of bonding and antibonding dangling bond states, because the Fermi level lies in the middle of the impurity band. He also proposed that the separation should be clearer when electron correlation is taken into account.

Detailed information about the influence of threefold-coordinated atoms on the electronic structure can be obtained by the computation of the corresponding LDOS. Mercer and Chou[41] and Biswas *et al.*[19] have analyzed the influence of defects utilizing the LDOS. We find that threefold-coordinated atoms give rise to a single peak between the two energy bands. This result is independent of the defect concentration and the system size and agrees with the work of Mercer and Chou. Biswas *et al.* found the formation of two peaks resulting from the dangling bonds. Unlike our structural model and the system studied by Mercer and Chou, Biswas *et al.* have taken into account an additional term in the Hamiltonian, the electron-electron interaction as realized in the Hubbard model (in the mean-field approximation). These authors, however, give no information about the structure of the LDOS when this interaction is switched off. Therefore it is difficult to compare to our results. Further differences between the structures used by Mercer and Chou and Biswas *et al.* are the defect concentrations and the relaxation potentials that are used to generate the amorphous structure. The structural model used by Mercer and Chou was obtained with the Stillinger-Weber potential and contains more dangling than floating bonds. The *a*-Si structure presented by Biswas *et al.* was generated with the two- and three-body Si potentials of Biswas and Hamann and contains the floating bonds as the dominant type of defect. A common feature of both structural models is the presence of dangling and floating bonds. We discuss in Sec. IV H that it is not easy to compare the LDOS obtained for different structural models, because the features in the LDOS of the threefold-coordinated atoms can be varied when different types of defects are present in the same structural model.

Schmitz[15] has also calculated the LDOS for threefold-coordinated atoms for his structural model, which is based on a quasicrystal. In common with our result and the result

TABLE II. Concentration of dangling and floating bonds for the WWW model in the case of relaxation with the Stillinger-Weber potential ($N=6$).

c_n	0.10	0.15	0.20	0.25
Dangling bonds	0.3%	1.0%	1.5%	2.4%
Floating bonds	2.2%	8.5%	16.4%	25.9%

TABLE III. Mobility gaps in eV for the defect structural models.

	$c_d=0$	$c_d=1.11$	$c_d=2.22$	$c_d=11.11$	$c_d=20$
DB model	2.0	2.5	2.3	0.5/1.5[a]	0.4/1.7[a]
FB model	2.0	1.81	2.0	0.5/0.5[a]	1.0[a]
DBFB model[b]	2.0	1.8	2.0	0.1/1.3[a]	0.3
WWW model+SW [c]	3.0 ($c_n=0.10$)	2.5 ($c_n=0.15$)	0.4 ($c_n=0.20$)	0 ($c_n=0.25$)	
a-Si:H	1.0	1.2	1.3	1.8	2.4

[a]See text.

[b]The structures contain just as many dangling bonds as floating bonds.

[c]WWW model in the case of relaxation with the Stillinger-Weber potential.

of Mercer and Chou the dangling bonds give rise to a single peak in the vicinity of the Fermi level. In his structural model, however, the threefold-coordinated atoms exclusively lead to states around the Fermi level. In the other energy regions the LDOS is negligibly small. This fact is in contrast to our result and the LDOS curves obtained by Mercer and Chou and Biswas *et al.*

In addition to atoms characterized by a coordination number of 3, with increasing defect concentration fourfold-coordinated atoms give rise to a small contribution to the DOS in the gap. These fourfold-coordinated atoms have one neighbor with a coordination number different from 4.

In comparison to the vacancy model the localization character of the states of the dangling bond model differs only in the region of the Fermi level. This means that this model shows stronger localization in the CB than in the VB. As long as the defect concentration is smaller than 11% all states in the region of the Fermi level are localized. For larger dangling bond concentrations we find a small amount of extended states between the two regions of localized states in the high-energy region of the VB as well as in the lower region of the CB. For all defect concentrations considered here the number of localized states in the region of the Fermi level is larger than at the bottom of the VB and the top of the CB. Through the introduction of dangling bonds the width of the mobility gap increases strongly compared to the vacancy model with the same degree of disorder. The value of the mobility gap shows no characteristic dependence on the defect concentration. If the defect concentration exceeds $c_d=10\%$ we can define two different mobility gaps (see Table III), due to the presence of extended states in the vicinity of the Fermi level.

E. Floating bond model

Similar to the introduction of threefold-coordinated atoms the presence of floating bonds leads to the formation of electronic states around the Fermi level (see Fig. 4). The number of states in this energy region is, however, smaller at the same concentration of defects compared to the dangling bond model. In contrast to the threefold-coordinated atoms the presence of floating bonds gives rise to additional states at the two outer band edges. The number of these states increases with increasing defect concentration. These changes are small compared to the effect found in the region of the Fermi level. The floating bond model behaves differently from the dangling bond model in another aspect: there is no strong dependence of the electronic structure on the system size.

The LDOS for the fivefold and sixfold-coordinated atoms is presented in the lower part of Fig. 4. Compared to the fourfold-coordinated atoms the floating bonds give rise to an

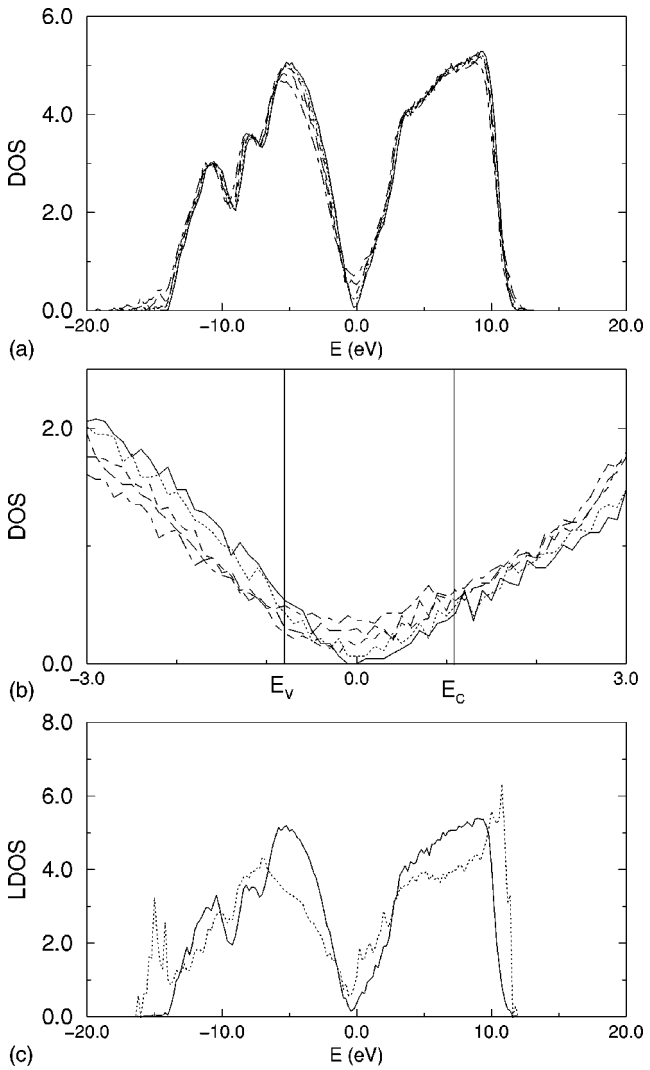

FIG. 4. Density of states (DOS) and local density of states (LDOS) for the floating bond model, (a) DOS, $N=6$ (1556 atoms) (solid line, $c_d=0\%$; dotted line, $c_d=1.11\%$; dashed line, $c_d=2.22\%$; long-dashed line, $c_d=11.11\%$; dash-dotted line, $c_d=20.0\%$). (b) DOS, $N=8$ (3688 atoms) (solid line, $c_d=0\%$; dotted line, $c_d=1.11\%$; dashed line, $c_d=2.22\%$; long-dashed line: $c_d=11.11\%$; dash-dotted line: $c_d=20.0\%$). (c) LDOS, $N=5$ (900 atoms), $c_d=11.11\%$ (solid line, fourfold-coordinated atoms; dotted line, fivefold- and sixfold-coordinated atoms).

additional peak at the top of the CB and at the bottom of the VB. The sixfold-coordinated atoms exert a stronger influence than the fivefold-coordinated ones. Whereas Mercer and Chou have found no differences in the LDOS between atoms with a tetrahedral coordination and the overcoordinated atoms, Biswas *et al.* have found characteristic features due to floating bonds. In agreement with our model they have observed that overcoordinated silicon atoms give rise to a larger number of electronic states in the region of the Fermi level and at the bottom of the VB compared to the fourfold-coordinated atoms. Analogously to the dangling bond model the number of states in the region of the Fermi level that arise from fourfold-coordinated atoms with a floating bond neighbor increases with the defect concentration. This feature was also observed by Mercer and Chou.

The states around the Fermi level are localized as long as the concentration of fivefold- and sixfold-coordinated atoms is smaller than $c_d = 11.11\%$. If the number of floating bonds exceeds this value a small amount of extended states arises in this energy region. For this type of defect the number of extended states is smaller than in the case of the dangling bonds. Whereas for all defect concentrations localized states exist at the bottom of the CB, we find localization at the top of the VB only for defect concentrations smaller than $c_d = 11.11\%$. In other words, we again find stronger localization at the bottom of the CB compared to the top of the VB. The width of the mobility gap increases with increasing defect concentration as long as the defect concentration is small, but its value is smaller than that for the dangling bond model (see Table III).

F. Dangling plus floating bond model

It is of particular interest to study the DOS of a structural model that contains both dangling and floating bonds. We observe the same features as in the models with only one type of defect, i.e., the effects turn out to be additive. Compared to the CRN we find more states in the vicinity of the Fermi level, at the bottom of the VB and at the top of the CB. Whereas the LDOS for the floating bonds in this structural model shows no differences to the pure floating bond model, the structure of the LDOS of the threefold-coordinated atoms exhibits small differences compared to the dangling bond model. For this type of defect the width of the peak in the LDOS increases with increasing defect concentration. The reason for this behavior is the simple fact that in this structural model two neighboring silicon atoms can both have a coordination number different from 4.

For this structural model the amount of localized states at the bottom of the VB and at the top of the CB increases with increasing defect concentration. In the vicinity of the Fermi level the number of localized states increases as long as the defect concentration is smaller than 11%. For larger defect concentrations we only observe localization at the bottom of the CB, similar to the models discussed above. The values of the mobility gaps for this structural model are listed in Table III. As long as the defect concentration is smaller than $c_d = 10\%$ the mobility gap increases with increasing defect concentration. If the number of undercoordinated and overcoordinated atoms is larger, the value of the mobility gap is smaller than for the CRN model and decreases with increasing defect concentration.

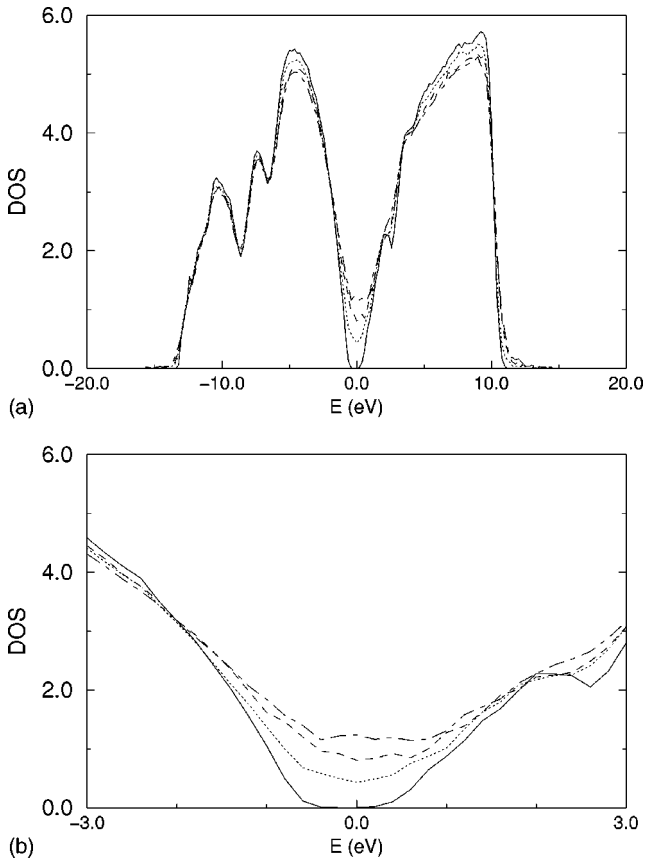

FIG. 5. Density of states for the double bond model, $N = 6$ (1556 atoms) (solid line, $c_d = 0\%$; dotted line, $c_d = 1.11\%$; dashed line, $c_d = 2.22\%$; dash-dotted line, $c_d = 11.11\%$). The energy resolution is in both cases 0.2 eV per interval.

G. Double bond model

Figure 5 shows the DOS of models containing double bonds. Compared to the CRN we observe two principal changes. This type of defect gives rise to a larger number of states at the bottom of the VB and at the top of the CB and leads to additional states in the vicinity of the Fermi level. In the latter energy region the number of states is larger than that for the floating bond model, but smaller than that for the dangling bond model. In contrast to the dangling bond model the DOS shows for no system size a peak at the Fermi level. The localization character of the states is nearly identical for both models containing threefold-coordinated atoms, i.e., the dangling bond and the double bond model.

H. Bond switching model combined with the Stillinger-Weber potential

In Fig. 6 we present the results obtained for the bond switching model, where the relaxation has been performed using the Stillinger-Weber instead of the Keating potential. Similar to the models described above the DOS becomes featureless with increasing disorder and the number of states in the vicinity of the Fermi level increases. For the same degree of disorder the number of states in the region of the Fermi level is larger than when the Keating potential is used. The explanation is simply that these structures contain both dangling and floating bonds. The upper edge of the VB lies at lower energies as compared to the Keating potential. For

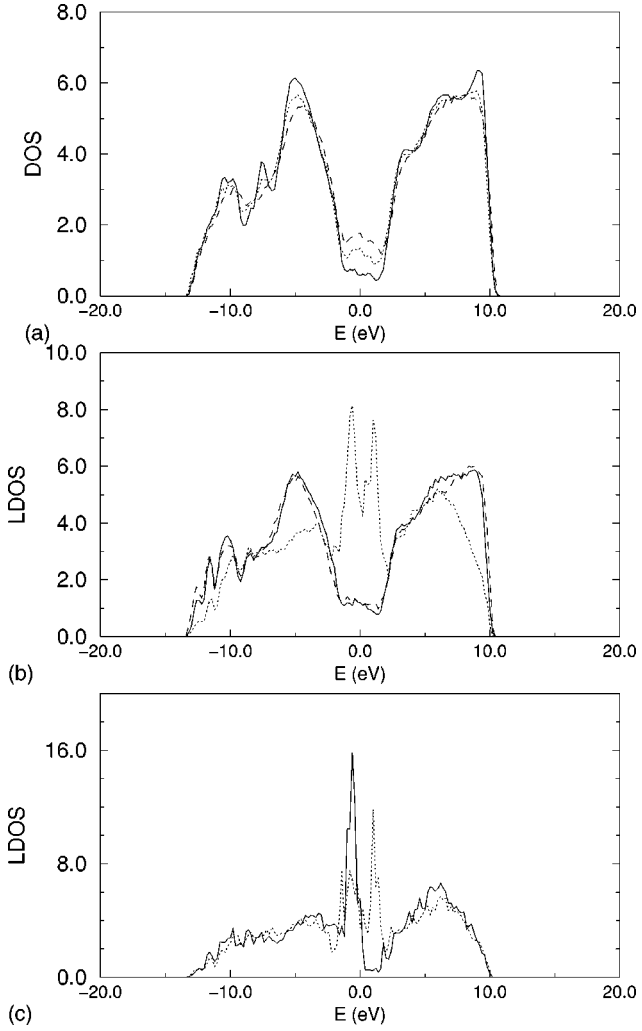

FIG. 6. Density of states (DOS) and local density of states (LDOS) in the case of relaxation with the Stillinger-Weber potential. (a) DOS, $N=6$ (solid line, $c_n=0.15$; dotted line, $c_n=0.20$; dashed line, $c_n=0.25$). (b) LDOS, $N=4$, $c_n=0.20$ (solid line, fourfold-coordinated atoms; dashed line, fivefold- and sixfold-coordinated atoms; dotted line, threefold-coordinated atoms). (c) LDOS, $N=4$, $c_n=0.20$ (solid line, threefold-coordinated atoms that are neighbors of fourfold-coordinated atoms; dashed line, threefold-coordinated atoms that have a fivefold- or sixfold-coordinated neighbor).

most of our calculations with the Stillinger-Weber potential we use a cutoff of 2.8 Å to generate the neighborhood list, and the resulting structures contain more floating than dangling bonds. Therefore the DOS shows no peak formation at the Fermi level. The concentration of the dangling and floating bonds for the various degrees of disorder is listed in Table II. If we calculate the DOS with a cutoff of 2.6 Å structures that contain more dangling than floating bonds are obtained. For these cases we find the formation of a small peak at the Fermi level for small system sizes. The DOS in the gap region obtained with our structural model and a cutoff of 2.8 Å is comparable with the results of Biswas *et al.* and of Mercer and Chou.

The LDOS for the different types of defects are shown in Fig. 6 (b). The curve for the fourfold coordinated atoms exhibits no essential difference compared to the other structural models and to those for fivefold- and sixfold-coordinated atoms. In contrast to the dangling bond model the LDOS of the threefold-coordinated atoms shows two peaks in the region of the Fermi level. An analysis shows that the peak at lower energies mainly arises from threefold-coordinated atoms that are neighbors of fourfold-coordinated ones. The second peak derives from threefold-coordinated atoms that have a neighbor with a coordination number different from 4. In the pure dangling bond model it is not possible that two neighboring atoms have both a coordination number different from 4 and therefore the peak in the vicinity of the Fermi level is not split.

Compared to the Keating potential the use of the Stillinger-Weber potential leads to a smaller amount of states that are localized at the two outer band edges. The number of states in this region shows no dependence on the degree of disorder. For a small degree of disorder the Stillinger-Weber potential leads to a larger amount of localized states in the region of the Fermi level. With increasing topological disorder and defect concentration the number of localized states decreases rapidly. If the disorder is smaller than $c_n=0.20$ we observe localization at the top of the VB and at the bottom of the CB. For a degree of disorder exceeding $c_n=0.20$ no localization is found at the top of the VB. For the highest degree of disorder ($c_n=0.25$) localized states are no longer present in the region of the Fermi level.

In addition to the structures based on the WWW model we have used molecular-dynamics simulations employing the Stillinger-Weber potential to generate structures of a-Si that contain 4096 and 216 atoms. To determine the neighborhood list we use a cutoff of 2.8 Å and obtain more floating than dangling bonds. The DOS of these structures gives no new aspects compared to the results of the WWW model together with the Stillinger-Weber potential. The LDOS of the overcoordinated and the undercoordinated atoms is also comparable with the results of the WWW model. In this case the structure of the LDOS of the threefold-coordinated atoms shows a dependence on its environment, whereas the LDOS of the overcoordinated atoms is nearly independent of the environment.

In addition to the models mentioned above we have generated a limited number of structures for the vacancy and the WWW model where the relaxation has been performed using the Tersoff potential.[49] The electronic properties (DOS and LDOS) of these structures are consistent with the results of the other structural models. In other words, the electronic structure of a-Si obtained in such a way can be understood as resulting in a nearly additive way from the models containing only dangling and only floating bond defects. This property also holds if the relaxation is done with the help of the Stillinger-Weber potential. An important difference between the structures generated with the Stillinger-Weber and the Tersoff potential lies in the ratio of the dangling bonds to floating bonds. Whereas the Stillinger-Weber potential leads to structures containing eight times more floating than dangling bonds, the use of the Tersoff potential leads to structures with a more balanced ratio of dangling bonds to floating bonds (1:3). The predominant formation of floating bonds in both cases is consistent with the results of the continuous-space MC simulations by Kelires and Tersoff.[11]

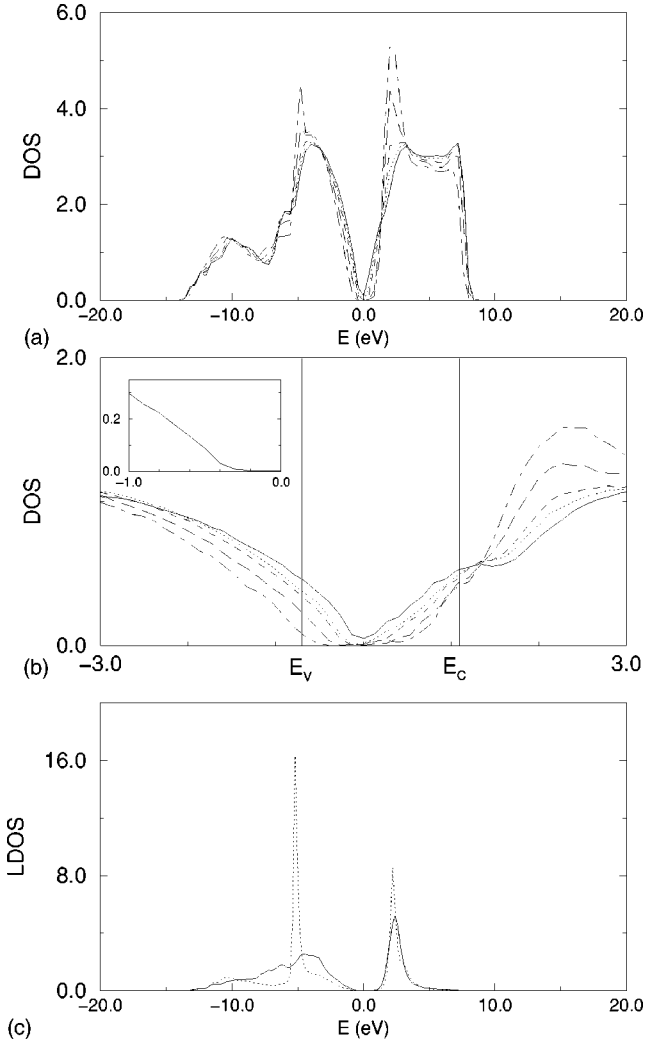

FIG. 7. Density of states (DOS) and local density of states (LDOS) for the *a*-Si:H model. (a) DOS, $N=6$ (1556 atoms). (b) DOS, $N=8$ (3688 atoms) (solid line, $c_H=0\%$, dotted line, $c_H=6.39\%$; dashed line, $c_H=12.24\%$; long-dashed line, $c_H=21.43\%$; dash-dotted line, $c_H=42.85\%$); inset, $c_H=21.43\%$. (c) LDOS, $N=5$ (900 atoms), $c_H=21.43\%$ (solid line, hydrogen in SiH_1 groups, dotted line, hydrogen in SiH_2 groups).

These authors estimated that the formation energies for fivefold-coordinated atoms are smaller than those for the threefold-coordinated ones.

I. *a*-Si:H model

In Fig. 7 we present the results for the *a*-Si:H model that is derived from the dangling bond model. If defects are partially removed from the structure by saturation with hydrogen, a strong decrease in the number of states in the vicinity of the Fermi level can be observed. Removing all defects leads to a true gap between the VB and the CB. The width of the gap increases with increasing amount of hydrogen. With increasing hydrogen concentration the formation of an additional peak at 2.8 eV above the Fermi level is observed. At the largest hydrogen concentration we observe a second peak at about 5 eV below the Fermi level. This maximum arises from hydrogen atoms which are bonded in SiH_2 and SiH_3 groups [see Fig. 7 (c)]. The formation of these two peaks in *a*-Si:H has also been found by Masek *et al.*[33] Various experiments[16,17] show that by the introduction of hydrogen the DOS is reduced at both the VB and the CB edge, with greater effect on the VB edge and the formation of a peak at 5 eV is observed. Our structural model is able to reproduce these effects. With increasing hydrogen concentration we additionally find that the top of the VB is shifted to lower energies by roughly 0.3 eV. This result agrees with experiment and other theoretical studies.[68–70,32,71,30] The bottom of the CB does not move with increasing hydrogen content. This result was also found in other calculations that are based on the tight-binding approach[69,70,30] but stands in contrast to some experimental measurements,[16,17] but is in agreement with the x-ray work of Sénémaud.[67] In photoemissions measurements the bottom of the CB recedes by about 0.2 eV. DiVincenzo, Bernholc, and Brodsky[71] have used the pseudopotential Green's function technique to determine the DOS and find a small shift of the CB edge.

Although we have used the same construction method as Holender, Morgan, and Jones our results are in some aspects different from theirs. In both structural models the introduction of hydrogen reduces the number of states in the gap region, but in the model developed by Holender, Morgan, and Jones the structure of the band edges is nearly independent of the hydrogen content. In both structural models the presence of hydrogen leads to a steeper increase of the DOS at the bottom of the CB than it is the case for *a*-Si. For our structural model the width of the energy gap is smaller than in the case of the model of Holender, Morgan, and Jones (0.64 eV compared to 1.2 eV) but the resulting mobility gaps are nearly identical and agree well with experiment. Figure 7(b) shows the DOS around the Fermi level for a structure containing 7200 atoms.

With the *a*-Si:H model we can reproduce the experimentally observed structure of the band tails. We can, however, only observe the linear part clearly [Fig. 7 (inset)]. The exponential tail is not clearly evident due to the noise, but a tailing behavior different from a linear one can be detected unambiguously.

The presence of hydrogen atoms causes no changes in the localization character of the states at the bottom of the VB and at the top of the CB. Just as for the other structural models mentioned above the *a*-Si:H model shows stronger localization at the bottom of the CB than at the top of the VB. Compared to the vacancy model the introduction of hydrogen leads to a widening of the mobility gap that agrees with experiment. The gap width increases with increasing hydrogen concentration (see Table III). If the hydrogen content in our model is close to the one found in real materials the value of the mobility gap (1.76 eV) is close to the experimental one (1.8 eV) and is comparable with the values obtained by Holender, Morgan, and Jones and by Schmitz.[15] Comparing the mobility gap of our structural model with that of Schmitz, it is necessary to note that the structure of Schmitz contains only silicon atoms. This author has generated two different structures (an unrelaxed tetrahedral quasicrystal and another one relaxed with the Keating potential). finding that the unrelaxed model can be compared with *a*-Si and the relaxed model with *a*-Si:H.

As we have observed differences in the tailing behavior between the vacancy model and the WWW model (see

above), we have generated a limited number of structures for *a*-Si:H that are based upon the bond switching model. The construction method is the same as for the vacancy model. In accord with the result for the CRN we are not able to reproduce the partition of the band edges into a linear and an exponential tail using the bond switching model. Thus the WWW model has some drawbacks with respect to the reproduction of the electronic structure compared to the vacancy CRN model and we conclude that the proper description of experiment leaves some work to be done. In these structures the introduction of hydrogen removes defect states from the gap region. Compared to the structures that are based on the vacancy model the shift of the valence-band edges is smaller for the WWW model and the bottom of the CB does not recede.

J. Microvoid model

The introduction of microvoids into the structures where the internal surfaces are saturated with hydrogen atoms does not lead to changes in the electronic structure compared to *a*-Si:H. This holds for both the DOS and for the localization character of the states and is independent of the size and the number of voids in the structure. As it is known that microvoids have a strong influence on transport properties we can only conclude that the DOS alone is insufficient to understand this effect.

V. CONCLUSIONS

In this paper we have presented the electronic density of states and the localization character of states for different structural models for *a*-Si and *a*-Si:H that contain essentially only one type of defect (dangling bonds, floating bonds, double bonds, saturation of dangling and floating bonds by hydrogen atoms, or microvoids). In addition to these models we have studied the properties of two different CRN's and a model containing both dangling and floating bonds. To obtain relaxed structures we have used a MC method utilizing the Keating potential. In some cases the Stillinger-Weber or the Tersoff potential and a molecular-dynamics approach have been applied. To calculate the DOS we have used a nearest-neighbor tight-binding approach. The localization properties are calculated with the TEL method, the scaling behavior of the correlation length and the IPR.

Before we assess the ability of the various structural models to reproduce the experimentally observed properties of *a*-Si and *a*-Si:H let us summarize the results obtained for the different structural models. All models discussed in this paper have a VB that consists of two peaks and in most cases a featureless CB. For the vacancy CRN model we find a true gap between the two energy bands that only fills up for unrealistically high vacancy concentrations. For the bond switching CRN model the gap disappears already at a small degree of disorder but the number of states in this region is still small. With increasing topological disorder the two energy bands lose their structure and the number of states in the vicinity of the Fermi level increases for both CRN's. In all structural models the introduction of different types of defects (dangling bonds, floating bonds, or double bonds) causes no strong changes in the principal structure of the two energy bands, but it leads to states in the vicinity of the Fermi level, and their number increases with increasing defect concentration. Dangling bonds induce more defect states in the gap region than floating bonds or double bonds do. Silicon atoms with a coordination number of five or six give rise to states at the bottom of the VB and at the top of the CB. The properties of systems containing overcoordinated atoms do not depend on the structural model or the relaxation potential. In contrast to this result the dangling bond model exhibits appreciable differences in its properties, once neighboring particles have a coordination number different from 4. The introduction of hydrogen removes all states around the Fermi level reintroducing a true gap and the VB edge recedes compared to the unhydrogenated form. Both the vacancy CRN model and the *a*-Si:H model are able to reproduce the experimentally observed tailing behavior (linear with an exponential tail). This behavior of the band edges is not found in the case of the bond switching model and the other defect models. It is neither found in an *a*-Si:H model derived from the bond switching model. This model thus exhibits some shortcomings.

All structural models discussed in this paper show stronger localization at the edges of the CB than at the VB edges. The states in the interior of the two energy bands seem to be extended. In the defect models the states in the vicinity of the Fermi level induced by dangling bonds, floating bonds, or double bonds are completely localized as long as the defect concentration is small, i.e., the atoms participating in a defect are essentially isolated in the structure. With increasing defect concentration the defects are no longer isolated and extended states form in the region of the Fermi level. The *a*-Si:H structure characterized by a hydrogen content of about 20 at. % shows a value of the mobility gap that is in good agreement with the experimental results. This is not the case for the pure CRN's and the defect models.

In contrast to the other types of defects the presence of microvoids causes no changes in the DOS and the localization character of the states compared to the simple *a*-Si:H model. Transport measurements, on the other hand, clearly demonstrate that microvoids exert a very strong influence.

Comparing the experimentally observed features of *a*-Si and *a*-Si:H to the results of the different structural models discussed in this paper we can assess the quality of the various models.

For *a*-Si the following experimental results are available: (a) The VB of the amorphous state consists of two peaks and the maximum of the upper peak lies at higher energies compared to the crystalline state. All structural models are able to reproduce these features. In most cases the width of the VB agrees with experiment; only the floating bond model gives a VB that is too wide by 1.6 eV. Compared to the experiment the upper peak of the VB is too wide for all structural models. The reason for this behavior lies in the tight-binding approach that is used to calculate the DOS, this is also known from the literature. (b) The featureless CB is reproduced with all defect models and the two CRN's with a realistic degree of topological disorder. (c) The experiment shows an asymmetry of the band edges in the gap region, i.e., for a given energy above and below the Fermi level the DOS is higher in the VB than in the CB. This behavior of the band edges is present in all structural models for *a*-Si. It is most evident in the double bond model and only weakly

apparent in the bond switching model combined with the Stillinger-Weber potential. This behavior of the DOS explains in a very satisfactory way that the VB states are less localized than the CB states. (d) In contrast to *c*-Si the density of states for *a*-Si shows states around the Fermi level. All defect models presented in this paper are able to reproduce the increased number of states in the vicinity of the Fermi level. (e) The mobility gap of *a*-Si has a value of $\sim$1.5 eV. None of the structural models is able to reproduce this value as long as the degree of topological disorder or the defect concentration is realistic.

Comparison between theory and experiment shows that no structural model is able to reproduce all experimentally observed features in the electronic properties. To describe the principal structure of the two energy bands and to study the influence of topological disorder the vacancy model and the bond switching model are both suitable. With the vacancy model a better description of the DOS in the vicinity of the Fermi level is possible. Therefore this structural model should be used to describe the electronic properties with a CRN. Finkemeier and von Niessen[46] have studied the vibrational properties of the two different CRN's and find that the bond switching CRN model is more suitable for this purpose. From this situation it is apparent that all models have still some unrealistic aspects. Models based upon *ab initio* MD simulations of the Car-Parrinello type, on the other hand, remain tiny due to the extreme computational demands. Due to the large cooling rates, defect concentrations are unrealistically high.

With the results presented in this paper we are certainly not able to answer the question of which type of defect is dominant in amorphous silicon or what role is played by the individual defects, but we have pointed out that dangling bonds have stronger influences on the electronic properties than the other types of defects. This result is independent of the structural model and the relaxation potential. This fact should also be contrasted to the results of Finkemeier and von Niessen on the phonon structure. They find considerable differences in the vibrational properties between the various structural models and between the relaxation potentials. For the case of the electronic properties we are not able to determine an ideal structural model for *a*-Si, because none of the structural models discussed in this paper is able to reproduce the experimentally observed DOS in the vicinity of the Fermi level in all its details. This implies that the DOS in this energy region originates from the interaction of the different types of defects or of additional interactions not included in the present work. It is difficult to model this situation because the individual defect concentrations are not known.

In all calculations presented in this paper the electron correlation is neglected. Elsewhere[72] we show how the properties of the various defect models change when this additional interaction is included. It will be presented that the introduction of the electron correlation leads to the formation of local magnetic moments on the dangling bond atoms, i.e., only this type of defect is ESR active. Therefore ESR experiments are able to determine only the dangling bond concentration. The real defect concentration in amorphous silicon lies probably above this value, because floating bonds have a smaller formation energy than dangling bonds but are ESR inactive and cannot easily be observed experimentally.

Comparing the results of the defect models obtained with the Keating and the Stillinger-Weber potential leads to the conclusion that the Keating potential is more suitable. The reason lies in the fact that the structures generated with the Stillinger-Weber potential show at a realistic degree of topological disorder defect concentrations exceeding appreciably the experimental concentration. This fact affects the localization character of the states more than the DOS does.

For the case of the *a*-Si:H model we are able to reproduce some important experimentally observed features, namely, the structure of the band tails, the receding of the VB edge, and the value of the mobility gap. Nevertheless our structural model is, for example, not able to reflect the receding of the CB edge. The reason for this fact may lie in the tight-binding approach that was used to calculate the DOS and the localization properties.

ACKNOWLEDGMENTS

Financial support by the Deutsche Forschungsgemeinschaft of S. K. and T. K., and partial support by the Fonds der Chemischen Industrie and the DAAD-ARC program are gratefully acknowledged. We thank F. Finkemeier for generating the structures of the WWW models and E. Oyen for making his molecular dynamics results available. We thank the computing center of the Technical University of Braunschweig, where the calculations have been performed on an IBM 3090/600 computer and on a Silicon Graphics Power Challenge XL, and the HLRZ Jülich for the supply of computing time on the CRAY T90.

[1] F. Wooten, K. Winer, and D. Weaire, Phys. Rev. Lett. **54**, 1392 (1985).
[2] D. Henderson and F. Herman, J. Non-Cryst. Solids **8-10**, 359 (1972).
[3] G. A. N. Connell and J. R. Temkin, Phys. Rev. B **9**, 5323 (1974).
[4] M. G. Duffy, D. S. Boudreaux, and D. E. Polk, J. Non-Cryst. Solids **15**, 435 (1974).
[5] D. L. Evans, M. P. Teter, and N. F. Borelli, J. Non-Cryst. Solids **17**, 245 (1975).
[6] R. Biswas, G. S. Grest, and C. M. Soukoulis, Phys. Rev. B **36**, 7437 (1987).
[7] W. D. Luedtke and U. Landman, Phys. Rev. B **40**, 1164 (1989).
[8] W. D. Luedtke and U. Landman, Phys. Rev. B **37**, 4656 (1988).
[9] M. D. Kluge, J. R. Ray, and A. Rahman, Phys. Rev. B **36**, 4234 (1987).
[10] J. Q. Broughton and X. P. Li, Phys. Rev. B **35**, 9120 (1987).
[11] P. C. Kelires and J. Tersoff, Phys. Rev. Lett. **61**, 562 (1988).
[12] R. Car and M. Parrinello, Phys. Rev. Lett. **60**, 204 (1988).
[13] D. A. Drabold, P. A. Fedders, O. F. Sankey, and J. D. Dow, Phys. Rev. B **42**, 5135 (1990).
[14] J. Schmitz, Z. Phys. B **100**, 75 (1996); J. Schmitz, J. Peters, and H. Trebin, *ibid.* **100**, 57 (1996); J. Schmitz, *ibid.* **100**, 63 (1996).
[15] J. Schmitz, *Ein Tetra-koordiniertes Quasiperiodisches Gitter als*

Modell Amorpher Halbleiter: Elektronische Zustände, Deutsche Hochschulschriften 463 (Egelsbach, Köln, 1993).
[16] *Hydrogenated Amorphous Silicon I*, edited by J. D. Joannopoulus and G. Lucovsky (Springer-Verlag, Berlin, 1984).
[17] *Hydrogenated Amorphous Silicon II*, edited by J. D. Joannopoulus and G. Lucovsky (Springer-Verlag, Berlin, 1984).
[18] C. S. Nichols and K. Winer, Phys. Rev. B **38**, 9850 (1985).
[19] R. Biswas, C. Z. Wang, C. T. Chan, K. M. Ho, and C. M. Soukoulis, Phys. Rev. Lett. **63**, 1491 (1989).
[20] Th. Koslowski and W. von Niessen, J. Phys.: Condens. Matter **4**, 6109 (1992).
[21] J. M. Holender and G. J. Morgan, J. Phys.: Condens. Matter **4**, 4473 (1992).
[22] R. A. Street, *Hydrogenated Amorphous Silicon* (Cambridge University Press, Cambridge, 1991).
[23] J. M. Holender, G. J. Morgan, and R. Jones, Phys. Rev. B **47**, 3991 (1993).
[24] D. Weaire and F. Wooten, J. Non-Cryst. Solids **35&36**, 495 (1980).
[25] L. Guttman, Phys. Rev. B **23**, 1866 (1981).
[26] Sh. Y. Ren and J. D. Dow, Phys. Rev. B **45**, 6492 (1992).
[27] F. Buda, G. L. Chiarotti, R. Car, and M. Parrinello, Phys. Rev. B **44**, 5908 (1991).
[28] I. Kwon, R. Biswas, and C. M. Soukoulis, Phys. Rev. B **45**, 3332 (1992).
[29] S. Wilke, J. Masek, and B. Velicky, Phys. Status Solidi B **135**, 309 (1986).
[30] W. Y. Ching, D. J. Lam, and C. C. Lin, Phys. Rev. Lett. **42**, 805 (1979); Phys. Rev. B **21**, 2378 (1980).
[31] B. J. Min, Y. H. Lee, C. Z. Wang, C. T. Chan, and K. M. Ho, Phys. Rev. B **45**, 6839 (1992).
[32] D. C. Allan and J. D. Joannopoulos, Phys. Rev. Lett. **44**, 43 (1980).
[33] J. Masek, V. Drchal, J. Malek, B. Velicky, and S. Wilke, J. Non-Cryst. Solids **77&78**, 87 (1985).
[34] D. Adler, B. B. Schwartz, and M. C. Steele, *Physical Properties of Amorphous Materials* (Plenum, New York, 1985).
[35] J. C. Phillips, Phys. Rev. Lett. **58**, 2824 (1987).
[36] M. Stutzmann and D. K. Biegelsen, Phys. Rev. Lett. **60**, 1682 (1988).
[37] P. A. Fedders and A. E. Carlsson, Phys. Rev. B **37**, 8506 (1988).
[38] P. A. Fedders and A. E. Carlsson, Phys. Rev. B **39**, 1134 (1989).
[39] S. T. Pantelides, Phys. Rev. Lett. **58**, 1344 (1987).
[40] J. H. Stathis, Phys. Rev. B **40**, 1232 (1989).
[41] J. L. Mercer, Jr. and M. Y. Chou, Phys. Rev. B **43**, 6768 (1991).
[42] J. M. Holender and G. J. Morgan, Modell. Simul. Mater. Sci. Eng. **2**, 1 (1994).
[43] K. Winer, I. Hirabayashi, and L. Ley, Phys. Rev. B **38**, 7680 (1988).
[44] K. Winer and L. Ley, Phys. Rev. B **36**, 6072 (1987).
[45] T. Tiedje, J. M. Cebulka, D. L. Morel, and B. Abeles, Phys. Rev. Lett. **46**, 1425 (1981).
[46] F. Finkemeier and W. von Niessen, following paper Phys. Rev. B **58**, 4473 (1998).
[47] P. N. Keating, Phys. Rev. **145**, 637 (1966).
[48] F. H. Stillinger and T. A. Weber, Phys. Rev. B **31**, 5262 (1985).
[49] J. Tersoff, Phys. Rev. B **38**, 9902 (1988).
[50] D. J. Chadi and M. C. Cohen, Phys. Status Solidi B **68**, 405 (1975).
[51] W. A. Harrison, *Electronic Structure and the Properties of Solids* (Freeman, San Francisco, 1980).
[52] S. C. Slater and G. F. Koster, Phys. Rev. **94**, 1498 (1954).
[53] P. Vogl, H. P. Hjalmarson, and J. D. Dow, J. Phys. Chem. Solids **44**, 365 (1983).
[54] P. A. Fedders and A. E. Carlsson, Phys. Rev. Lett. **58**, 1156 (1987).
[55] P. B. Allen, J. Q. Broughton, and A. K. McMahan, Phys. Rev. B **34**, 859 (1986).
[56] D. C. Allan and E. J. Mele, Phys. Rev. B **31**, 5565 (1985).
[57] S. R. Elliot, *Physics of Amorphous Materials* (Longman, London, 1989).
[58] T. M. Chang, J. D. Bauer, and J. L. Skinner, J. Chem. Phys. **93**, 8973 (1990).
[59] D. E. Sigeti, Xiodang Zhang, M. S. Friedrich, and R. A. Friesner, Phys. Rev. B **44**, 614 (1991).
[60] D. C. Licciardello and D. J. Thouless, J. Phys. C **8**, 4157 (1975).
[61] J. T. Edwards and D. J. Thouless, J. Phys. C **5**, 807 (1972).
[62] D. C. Licciardello and D. J. Thouless, J. Phys. C **11**, 925 (1978).
[63] Th. Koslowski and W. von Niessen, J. Comput. Chem. **14**, 769 (1993).
[64] L. Lanczos, J. Res. Nat. Bur. Stand. Sect. B **45**, 225 (1980).
[65] K. Cullman and R. Willoughby, *Lanczos Algorithms for Large Symmetric Eigenvalue Problems Vol. I, Theory* (Birkhäuser, Boston, 1985); K. Cullman and R. Willoughby, *Lanczos Algorithms for Large Symmetric Eigenvalue Problems Vol. II, Programs* (Birkhäuser, Boston, 1985).
[66] R. Bellissent, A. Chenevas-Paule, P. Chieux, and A. Menelle, J. Non-Cryst. Solids **77&78**, 213 (1985).
[67] C. Sénémaud, J. Non-Cryst. Solids **198-200**, 85 (1996).
[68] V. Drchal and J. Malek, J. Non-Cryst. Solids **90**, 103 (1987).
[69] E. N. Economou and D. A. Papaconstantopoulos, Phys. Rev. B **23**, 2042 (1981).
[70] D. C. Allan, J. D. Joannopoulos, and W. B. Pollard, Phys. Rev. B **25**, 1065 (1982).
[71] D. P. DiVincenzo, J. Bernholc, and M. H. Brodsky, Phys. Rev. B **28**, 3246 (1983).
[72] S. Knief and W. von Niessen (unpublished).